scientific reports

Check for updates

OPEN

Concurrent tDCS-fMRI after stroke reveals link between attention network organization and motor improvement

Claudia A. Salazar[1,2], James M. Welsh[1,2], Daniel Lench[3], Irene E. Harmsen[4], Jens H. Jensen[2,5], Parneet Grewal[3], Milad Yazdani[6], Sami Al Kasab[1,3], Alex Spiotta[1,3], Leonardo Bonilha[7], Mark S. George[2,3,5,8,9,10], Steven A. Kautz[8,11] & Nathan C. Rowland[1,2,3,8,11]✉

Restoring motor function after stroke necessitates involvement of numerous cognitive systems. However, the impact of damage to motor and cognitive network organization on recovery is not well understood. To discover correlates of successful recovery, we explored imaging characteristics in chronic stroke subjects by combining noninvasive brain stimulation and fMRI. Twenty stroke survivors (6 months or more after stroke) were randomly assigned to a single session of transcranial direct current stimulation (tDCS) or sham during image acquisition. Twenty healthy subjects were included as controls. tDCS was limited to 10 min at 2 mA to serve as a mode of network modulation rather than therapeutic delivery. Fugl-Meyer Assessments (FMA) revealed significant motor improvement in the chronic stroke group receiving active stimulation ($p = 0.0005$). Motor changes in this group were correlated in a data-driven fashion with imaging features, including functional connectivity (FC), surface-based morphometry, electric field modeling and network topology, focusing on relevant regions of interest. We observed stimulation-related changes in FC in supplementary motor ($p = 0.0029$), inferior frontal gyrus ($p = 0.0058$), and temporo-occipital ($p = 0.0095$) areas, though these were not directly related to motor improvement. The feature most strongly associated with FMA improvement in the chronic stroke cohort was graph topology of the dorsal attention network (DAN), one of the regions surveyed and one with direct connections to each of the areas with FC changes. Chronic stroke subjects with a greater degree of motor improvement had lower signal transmission cost through the DAN ($p = 0.029$). While the study was limited by a small stroke cohort with moderate severity and variable lesion location, these results nevertheless suggest a top-down role for higher order areas such as attention in helping to orchestrate the stroke recovery process.

Recovery from stroke is highly dynamic and involves an elaborate interplay among motor and cognitive systems[1–3]. This is reflected in the multi-modal deficits that occur in a large proportion of stroke patients, for example, those with comorbid motor and language impairments. Consequently, a promising therapeutic trend has emerged that emphasizes an integrated, multi-domain approach to stroke rehabilitation[4]. However, the theoretical basis for such an approach is currently lacking, and no mechanism has been proposed to explain how a trans-disciplinary framework is likely to benefit patients suffering from various stroke-related syndromes.

[1]Department of Neurosurgery, College of Medicine, Medical University of South Carolina, 96 Jonathan Lucas St., CSB301 MSC606, Charleston, SC 29425, USA. [2]Department of Neuroscience, College of Graduate Studies, Medical University of South Carolina, Charleston, SC, USA. [3]Department of Neurology, College of Medicine, Medical University of South Carolina, Charleston, SC, USA. [4]Division of Neurosurgery, Department of Surgery, Toronto Western Hospital, University of Toronto, Toronto, ON, Canada. [5]Center for Biomedical Imaging, Medical University of South Carolina, Charleston, SC, USA. [6]Department of Radiology and Radiological Science, College of Medicine, Medical University of South Carolina, Charleston, SC, USA. [7]Department of Neurology, College of Medicine, University of South Carolina, Columbia, SC, USA. [8]Department of Health Sciences and Research, College of Health Professions, Medical University of South Carolina, Charleston, SC, USA. [9]Ralph H. Johnson VA Medical Center, Charleston, SC, USA. [10]Department of Psychiatry, College of Medicine, Medical University of South Carolina, Charleston, SC, USA. [11]MUSC Institute for Neuroscience Discovery (MIND), Medical University of South Carolina, Charleston, SC, USA. ✉email: rowlandn@musc.edu

Based on a growing body of new data[5], many investigators have begun to question whether stroke-related neuroplasticity in motor and cognitive networks occurs independently or in tandem. Connections between the two sets of systems are numerous. For instance, the supplementary motor area (SMA), which serves pre-motor functions, is also active during speech comprehension, grammar and articulation[6]. Moreover, a portion of SMA output fibers synapses directly onto language-related cortical areas in inferior frontal gyrus (IFG) via the frontal aslant fiber tract[7]. In a resting state functional imaging study of patients with moyamoya disease, a correlation was observed between SMA-IFG functional connectivity (FC) and performance on cognitive assessments[8]. Interestingly, IFG activity has also been linked to visual observation of the same spoken motor task[9,10]. Thus, clinical, anatomical and imaging evidence suggest tight integration of multiple areas, though whether SMA, IFG or the various connections between them drive motor improvement in stroke is not well agreed upon.

Non-invasive brain stimulation, which can be delivered to specific brain regions and networks, transiently improves stroke outcomes in a number of domains when paired with rehabilitation. In a recent study, transcranial direct current stimulation (tDCS) was used to target the prefrontal cortex in patients with aphasia while undergoing language testing. The authors reported improvement in grammar acquisition along with enhanced performance in sustained attention[11]. Given that SMA and IFG are implicated in the two dominant attention pathways, i.e., the dorsal and ventral attention systems, respectively, these results raise the intriguing possibility that large-scale attention networks could be exploited to better target certain types of stroke recovery. Attention networks are known to be cross-modal and to permit dynamic overlap of functionally related executive processes. Since it is well accepted that motor rehabilitation depends on intact visuo-spatial, language and attention processing, the idea that multiple systems synchronize during recovery aligns well with clinical experience.

In the current study, using tDCS effect on upper extremity motor performance, we aimed to determine whether motor recovery in chronic stroke is associated with changes in functional brain regions such as SMA and IFG or whether such changes are driven by large-scale cognitive networks like those involved in attention. To test this, we performed functional magnetic resonance imaging (fMRI) in ten subjects with chronic stroke undergoing motor cortical tDCS, while an additional ten stroke subjects received sham stimulation[12–14]. Twenty healthy subjects (20) were included as controls. Fugl-Meyer Assessment (FMA) scores were measured before and after imaging in all subjects. tDCS was employed as a mode of network modulation during a single session rather than therapeutic means. Brain regions and networks related to motor and cognitive function were surveyed for changes in functional connectivity, surface-based morphometry, electric field modeling and network topology in relation to motor improvement. This study represents an important step towards establishing the role of image-guided biomarkers of adaptive network reorganization in stroke recovery.

Results

Baseline demographics

Forty subjects (20 healthy controls and 20 chronic stroke patients) completed the study protocol and were included in the data analysis. The time between stroke and study participation ranged from 6 to 88 months (median = 38 months). There were no significant differences between the healthy control (HC) and chronic stroke groups for mean age ($p = 0.6352$, $t_{[38]} = -0.47822$) or sex ($p = 0.2036$, $\chi^2_{[1]} = 1.6162$). Similarly, there were no significant differences between the chronic stroke stimulation (hereafter referred to as stim) and sham groups for mean age ($p = 0.0895$, $t_{[18]} = 1.795$) or sex ($p = 0.6531$, $\chi^2_{[1]} = 0.202$). There were no significant differences between lesion size or time since stroke between the stroke stim and stroke sham groups (lesion size: $p = 0.6473$, $t_{[18]} = 0.4653$; time since stroke: $p = 0.8256$, $t_{[19]} = 0.000$). A statistically significant difference was observed between the chronic stroke stim and sham groups for mean National Institutes of Health Stroke Scale (NIHSS) scores at the time of admission ($p = 0.0987$, $t_{[14]} = -1.788$; stim: 10.1 ± 6.1, sham: 5.4 ± 6.1) and discharge ($p = 0.0084$, $t_{[15]} = 3.029$, stim: 6.1 ± 5.2, sham: 2.5 ± 2.4). Thus, the chronic stroke stim group exhibited more severe symptoms at both time points. See Tables 1 and 2 for full demographic profiles.

Uniform tDCS dosing improved FMA scores in the chronic stroke group despite heterogeneous lesion size and location

To determine the effect of tDCS on upper extremity movement in our cohort, the Fugl-Meyer Assessment Upper Extremity (FMA-UE) scale was administered before and after stimulation for all subjects. There were no statistically significant differences in FMA-UE scores pre- to post-stimulation in the HC groups (*stim*: no calculable p value given that identical pre- and post-stim values were observed within each subject; *sham*: $p = 0.3434$, $t_{[9]} = 1$, Fig. 1a). There was a statistically significant mean increase of 8.1 points in FMA-UE scores from pre- to post-stimulation in the stroke stim group ($p = 0.0005$, $t_{[9]} = 5.2914$, Fig. 1a). There was no statistically significant difference in FMA-UE scores from pre- to post-stimulation in the stroke sham group ($p = 0.3270$, $t_{[9]} = 1.037$). Thus, improvement in FMA-UE scores exceeded the threshold for minimal clinically important difference in the stroke stim group only[15,16]. To rule out the possibility that the observed improvements were influenced by subject-related factors, we performed a linear regression between time since stroke and change in FMA-UE from pre- to post-tDCS among both stroke groups and found no association (*stim*: $p = 0.4652$, $r^2_{[8]} = 0.9972$, *sham*: $p = 0.3945$, $r^2_{[8]} = 0.9849$). Moreover, there were no statistically significant associations between lesion size and change in FMA-UE score (*stim*: $p = 0.4652$, $r^2_{[8]} = 0.065$, *sham*: $p = 0.3945$, $r^2_{[7]} = 0.0919$). Hence, improvement in FMA-UE in the chronic stroke stim group was not related to shorter disease duration or smaller extent of stroke.

Within the stroke stim group, 7/10 subjects demonstrated improvement of one or two points in both the flexor synergy and hand items FMA subdomains. In the speed and coordination, wrist items, and out of synergy subdomains, 6/10, 5/10, and 5/10 subjects, respectively, improved by one point. In the extensor synergy and combining synergy subdomains, 3/10 and 2/10 subjects improved by one point. The following subdomains demonstrated decreases by one point: out of synergy, wrist items, hand items, and speed and coordination. Taken together,

ID	Group	Stim status	Age	Sex	Stroke type	Lesion size (cm^3)	Vascular territory	Stroke laterality	Time since stroke (months)	NIHSS at admission	NIHSS at discharge
2	Stroke	Stim	49	F	Hemorrhagic	13.39	mca	Left	19	21	15
5	Stroke	Stim	53	M	Ischemic	79.58	Vertebral artery	Left	80	6	5
19	Stroke	Stim	47	M	Hemorrhagic	1.13	pca	Left	88	13	9
24	Stroke	Stim	62	F	Ischemic	0.93	pca	Right	57	–	–
25	Stroke	Stim	60	M	Hemorrhagic	145.59	mca/pca	Right	81	7	4
33	Stroke	Stim	50	M	Ischemic	120.53	mca	Right	6	13	10
34	Stroke	Stim	52	M	Hemorrhagic	6.62	mca	Left	22	19	3
36	Stroke	Stim	61	M	Ischemic	2.07	mca/ica	Right	16	6	5
37	Stroke	Stim	42	F	Hemorrhagic	0.10	aca	Left	38	2	0
40	Stroke	Stim	60	F	Ischemic	42.83	mca	Right	17	9	5
12	Stroke	Sham	63	F	Ischemic	46.77	mca	Left	11	3	-
17	Stroke	Sham	75	M	Ischemic	18.94	Vertebral artery	Left	77	1	1
23	Stroke	Sham	77	M	Unknown	77.39	Unknown	Left	80	–	–
28	Stroke	Sham	84	M	Ischemic	0.23	Vertebral artery	Right	81	1	0
29	Stroke	Sham	70	F	Hemorrhagic	1.54	aca	Right	20	1	1
32	Stroke	Sham	60	M	Ischemic	17.57	Basilar	Right	16	4	4
35	Stroke	Sham	60	F	Ischemic	15.57	mca	Right	8	8	3
38	Stroke	Sham	47	F	Ischemic	37.81	mca	Right	14	3	1
39	Stroke	Sham	43	F	Ischemic	0.28	Multiple	Right	6	–	–
42	Stroke	Sham	46	M	Hemorrhagic	3.06	mca	Right	78	–	–

Table 1. Individual demographics of stroke subjects. *NIHSS* National Institutes of Health Stroke Scale, *HC* healthy control, *Stim* stimulation, *F* female, *M* male.

	Age years ± SD	Race n (%)	Hispanic/Latino n (%)	Sex F/M
Healthy controls (N = 20)				
Stim (n = 10)	57.1 ± 16.7	7 (70%) Caucasian 3 (30%) African American	0 (0%)	F: 9 M: 1
Sham (n = 10)	64.7 ± 13.5	6 (60%) Caucasian 3 (30%) Other 1 (10%) African American	2 (20%)	F: 4 M: 6
Stroke survivors (N = 20)				
Stim (n = 10)	53.6 ± 6.5	7 (70%) African American 1 (10%) Caucasian 1 (10%) Pacific Islander 1 (10%) Asian	0 (0%)	F: 4 M: 6
Sham (n = 10)	62.4 ± 12.7	7 (70%) African American 3 (30%) Caucasian	0 (0%)	F: 5 M: 5

Table 2. Group demographics of all study subjects. *Stim* stimulation, *F* female, *M* male, *n* number, *SD* standard deviation.

the change in FMA-UE was broadly distributed across domains and subdomains in the stroke stim group (Supplementary Fig. 1). In contrast, within the stroke sham group, only 2/10 subjects demonstrated improvement of one point in both the out of synergy and speed and coordination subdomains. In the flexor synergy, wrist item, and speed and coordination subdomains, 1/10 subjects improved by one point. In the hand items, combining synergy, and extensor synergy subdomains, 2/10, 2/10, and 1/10 subjects, respectively, decreased by one point. Thus, the stroke sham group experienced a more sparse distribution of changes (Supplementary Fig. 1).

In order to assess variation specifically in hand movement and finger dexterity as a function of tDCS, we administered the nine-hole peg test (NHPT) to subjects in the stroke group. In this test, a shorter duration to insert all 9 pegs implies quicker performance. There was a significant decrease in the mean completion time for the stroke stim group from pre- to post-stimulation ($p = 0.0017$, $t_{[5]} = 5.196$, Fig. 1b) but not for the sham group ($p = 0.6885$, $t_{[6]} = 0.4209$). Performance on the NHPT did not appear to be related to pre-stimulation severity of hand function, given that there was no statistically significant difference between the stroke stim and sham pre-stimulation NHPT values ($p > 0.05$).

In addition to FMA-UE and NHPT, which were performed in an external treatment room, all subjects completed a finger-sequencing task while inside the MRI scanner. A 2-factor ANOVA revealed no statistically significant differences in number of correct sequences over time for either stroke stim or stroke sham groups (*time*: $p = 0.695$, $f[2, 24] = 0.37$; *stim vs sham*: $p = 0.223$, $f[1, 24] = 1.57$; *time* × *stim vs sham interaction*: $p = 0.967$,

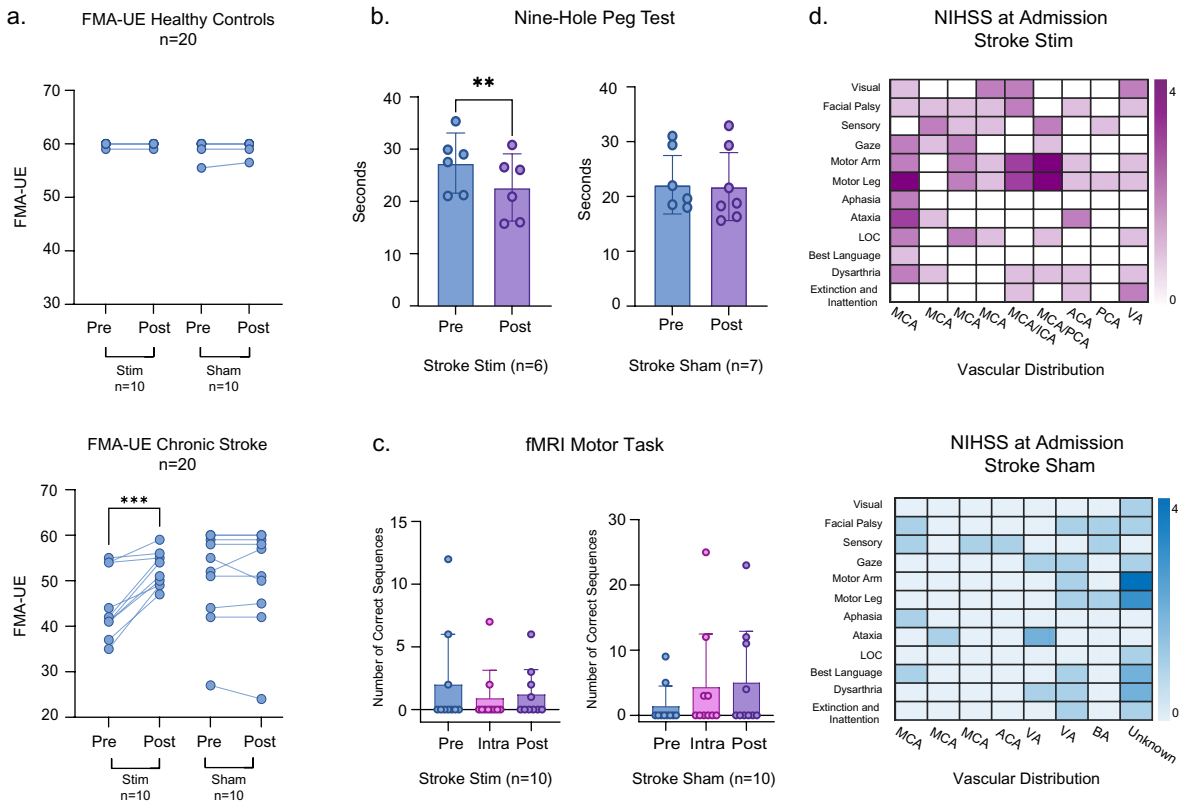

Figure 1. (**a**) FMA-UE scores were collected for all subjects and analyzed based on their respective group assignments (HC stim = 10; HC sham = 10; chronic stroke stim = 10; chronic stroke sham = 10). The first column represents individual FMA-UE scores before and after stimulation. (**b**) Bar graphs represent the nine-hole peg test scores for the stroke stim (n = 6) and stroke sham (n = 7) groups. The graphs show individual values, mean, and 95% confidence intervals. Pre-stimulation (*blue*) and post-stimulation (*purple*) scores are shown. (**c**) All subjects completed a finger-tapping task while inside the MRI scanner. The plots represent the number of correct sequences achieved at each timepoint (pre, intra, post) and include 95% confidence intervals for chronic stroke stim (n = 10) and sham (n = 10) groups. (**d**) NIHSS scores are shown as a heat map for chronic stroke stim (magenta) and chronic stroke sham (blue). NIHSS domains are represented in the y axis and vascular distributions are shown along the x axis. Each vertical column represents one subject. Three subjects are not represented in the heat map (1 chronic stroke stim, 2 chronic stroke sham) due to inaccessible NIHSS scores. *ACA* anterior cerebral artery, *BA* basilar artery, *ICA* internal carotid artery, *LOC* loss of consciousness, *MCA* middle cerebral artery, *PCA* posterior cerebral artery, *VA* vertebral artery.

$f[2, 24] = 0.03$, Fig. 1c). This result was similar for the healthy control groups. Thus, while tDCS did improve finger movement dexterity, it did not improve finger movement speed, particularly with regard to sequencing, even in healthy controls. Importantly, improvement in FMA-UE and NHPT was accomplished using uniform dosing and montage placement for all chronic stroke subjects that received active stimulation, despite this group having variable stroke lesion size and type (Fig. 1d) and being more clinically affected than the sham group.

Functional connectivity changes in motor and cognitive regions following stimulation were aligned with differences in cortical morphometry and electric field modeling

To test the hypothesis that motor improvement in the stroke stim group was related to changes in whole brain connectivity, functional connectivity (FC, hereafter referred to as connectivity) was measured for all individual regions of interest (total of 164 Harvard–Oxford-AAL atlas designations) in relation to averaged connectedness with all other regions (see Methods and Supplementary Table 1 for full listing of ROIs). Subtracting the pre- and post-stimulation time periods, the left supplementary motor area (L SMA) emerged as the region with the highest positive connectivity change for stroke stim subjects (Fig. 2a–d). Interestingly, functional color-coding of the bars showed that connectivity for sensorimotor areas (green) on average dispersed toward more positive values over time, while those for language (magenta) and visual (blue) regions shifted toward more negative values. Areas involved in attention processing (orange)—including the dorsal attention network (of which there were 4 atlas sub-designations: left/right intraparietal sulcus (DAN IPS) and left/right frontal eye fields (DAN FEF))—exhibited positive changes over time but at an attenuated rate compared to sensorimotor regions (Fig. 2a–d).

Given the change in L SMA connectivity in our cohort, to rule out sampling bias we explored whether the laterality of SMA connectivity change depended on the side of the affected hemisphere (i.e., left vs right). Figure 2e shows that in the stroke group, left ipsilesional anodal stimulation resulted in increases in L SMA connectivity

with approximately the same frequency as right ipsilesional anodal stimulation. In contrast, in the healthy control group, left anodal stimulation resulted primarily in a decrease in L SMA connectivity regardless of stimulation status. Figure 2f displays examples of connectogram changes in L SMA connectivity for individual stroke stim and stroke sham subjects, pre- and post-tDCS administration.

In order to determine whether functional connectivity varied statistically as a function of tDCS, we examined connectivity data of all 164 regions at the three stimulation timepoints (i.e., pre-, intra-, and post-stimulation). Between the pre- and post-stim periods, L SMA connectivity was observed to increase significantly for the stroke stim ($p = 0.0029$, $t_{[18]} = 3.463$) but not stroke sham group ($p = 0.8571$, $t_{[18]} = 0.1552$, Fig. 2g). Of the additional 163 regions examined for changes in mean connectivity across pre-, intra-, and post-tDCS timepoints, only 3 other regions, all on the left side and all of which are involved in language and visual processing, showed statistical significance in the stroke stim group only (corrected using false discovery rate or fdr, see Supplementary Table 2 and "Statistical analysis"). Importantly, the left dorsal attention network did not show significant change in connectivity between the pre and post-stimulation timepoints ($p = 0.840$, $t_{[18]} = 0.1552$). See Supplementary Figs. 3 and 4 for raw connectivity matrices).

Because our stroke cohort was not limited to a specific lesion location or size (Fig. 3a–c), we sought to rule out the influence of individual variability in cortical damage on tDCS efficacy. However, mean whole brain cortical thickness did not differ between chronic stroke stim and sham groups (*stim:* 2.32 ± 0.11; *sham:* 2.285 ± 0.12, $p = 0.5709$, $t_{[16]} = 0.5787$), suggesting that sham subjects' overall failure to improve was unlikely due to a higher burden of cortical damage. As a control for the sensitivity of mean cortical thickness to vary between disease states, we compared mean whole brain cortical thickness between HC and chronic stroke groups and observed a statistically significant overall difference (*HC*: 2.42 ± 0.09, *CS*: 2.32 ± 0.10, $p = 0.0041$, $t_{[36]} = 3.071$, Fig. 3d). Interestingly, differences in cortical thickness between HC and chronic stroke groups were restricted to motor, language and visual regions (see fdr-corrected values in Supplementary Table 3).

In previous studies, cortical thickness has been directly linked to tDCS efficacy based on the rationale that parenchymal density influences electric field (EF) strength[17,18]. Thus, to rule out differences in EF strength between the two stroke groups, we modeled regional EFs using bihemispheric tDCS montages and observed that maximum EF strength was greatest at the supramarginal gyrus, a key parietal region, for all stroke subjects, rather than at motor cortical regions closer to the anode such as the SMA as expected. Nevertheless, there was no significant difference in mean maximum EF strength of the supramarginal gyrus between chronic stroke stim and sham groups (left supramarginal gyrus: $p = 0.5217$, $t_{[17]} = 0.6543$; right supramarginal gyrus: $p = 0.4058$, $t_{[17]} = 0.8526$, Fig. 3e,f).

Notwithstanding these observations, FMA-UE change in chronic stroke stim subjects was not explained by change in connectivity (L SMA, pre vs post: $p = 0.486$, $r^2_{[8]} = 0.0626$) or mean whole brain cortical thickness ($p = 0.0640$, $r^2_{[8]} = 0.4082$). Maximum EF strength at the supramarginal gyrus was also not correlated with FMA-UE change in the stroke stim group (left: $p = 0.4729$, $r^2_{[18]} = 0.076$; right: $p = 0.5993$, $r^2_{[18]} = 0.041$). Thus, while motor, language and visual area changes were associated with active stimulation in the stroke group, neither functional connectivity, cortical surface morphometry or EF dynamics independently influenced motor behavioral improvement. These metrics were similarly ineffective in explaining FMA-UE change for the four dorsal attention network ROIs ($p > 0.05$).

Attention network topology accounted for variability in motor improvement in stroke subjects

To test the hypothesis that whole-brain network topology influences motor improvement with tDCS, we computed the following graph theoretic measures for a subset of ROIs in all subjects (see "Methods" and Supplementary Table 4): average path length, clustering coefficient, local efficiency, global efficiency, betweenness centrality, cost, and degree centrality. For the chronic stroke subjects, permutations between group assignment, graph theory metric and ROI yielded numerous significant pre-post stimulation changes associated with change in FMA-UE. Hence, to address whether these observations were specifically associated with tDCS administration or were related to the chronic stroke disease state, we combined the stroke stim and sham subjects into one group and noted that many of the correlations survived pooling (Supplementary Table 4, middle 2 columns, corrected using modified multi-threshold permutation correction). A subset of areas remained strong enough that the pre-stimulation network state (i.e., prior to administering tDCS) remained significantly correlated with the change in FMA-UE (Supplementary Table 4, last column, corrected using modified multi-threshold permutation correction). The network with the strongest correlation between pre-stimulation cost and FMA-UE change was the L dorsal attention network intraparietal sulcus (L DAN IPS, $p = 0.029$, $r^2_{[18]} = 0.2811$). Cost, which reflects the metabolic expenditure of signal transmission, was lower in subjects who exhibited higher FMA change (Fig. 3g). FMA-UE change across both stroke groups was also correlated with L DAN IPS pre-stimulation betweenness centrality ($p = 0.041$, $r^2_{[18]} = 0.2432$), global efficiency ($p = 0.031$, $r^2_{[18]} = 0.2386$) and degree centrality ($p = 0.029$, $r^2_{[18]} = 0.2811$). Degree centrality plays a primary role in network behavior as it identifies network hubs. Importantly, we identified the 2 stroke sham subjects with spontaneously improved FMA-UE using pre-stimulation L DAN IPS network metrics alone (Fig. 3g, n.b. red circles). These data suggest that motor response to tDCS can potentially be linked to task-based fMRI measurement of network topology even in the absence of stimulation, an important methodological consideration for future studies.

Discussion

Our study aimed to uncover the regional and network imaging features linked to motor improvement in chronic stroke survivors. Despite a broad sampling of stroke territories and sizes, FMA-UE significantly improved in all chronic stroke subjects receiving active tDCS, the only group to experience such change. In this group, functional connectivity alterations in SMA (motor), IFG (language) and TO (vision) were observed with tDCS, however

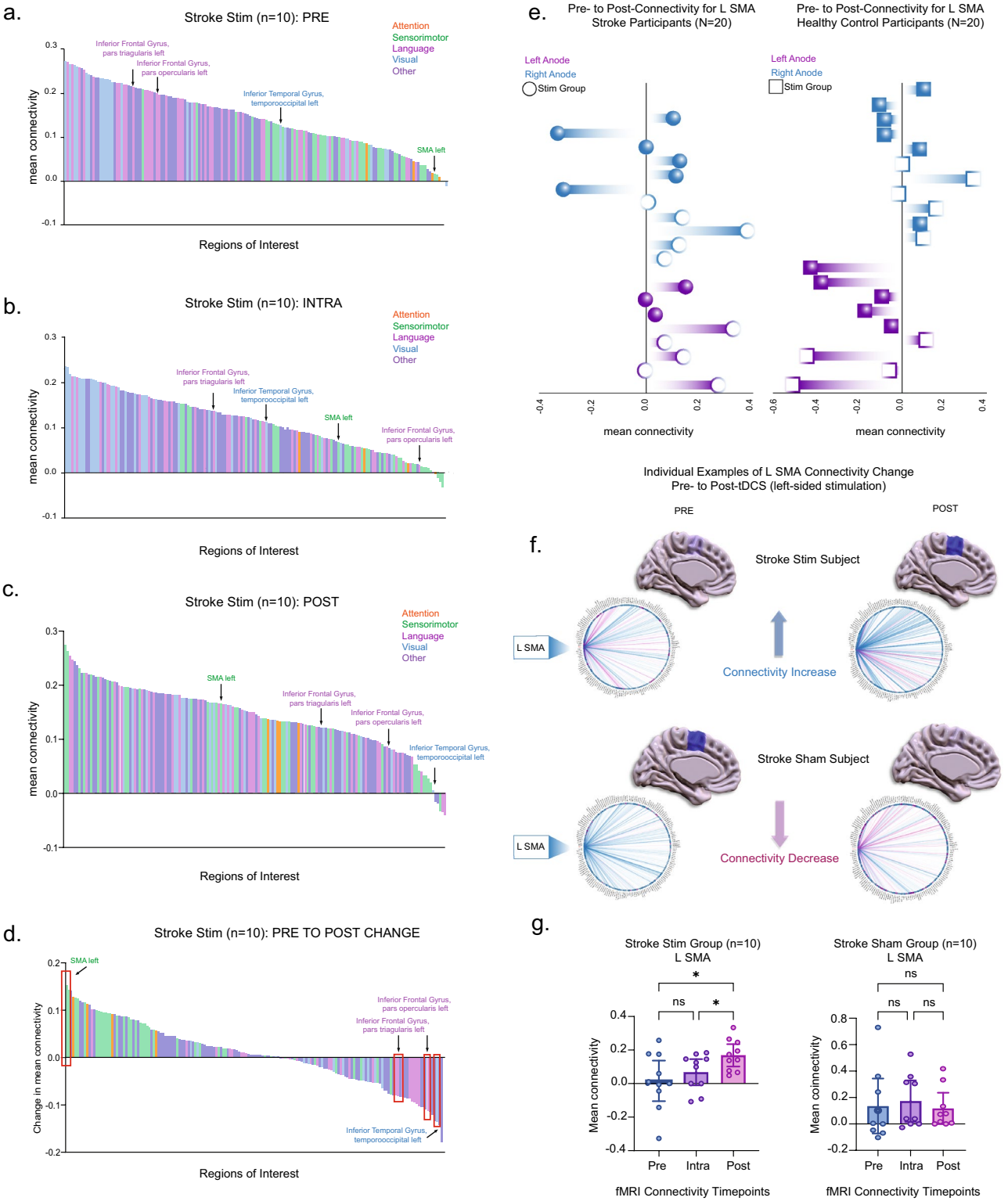

these isolated changes were not independently associated with motor improvement. Instead, FMA-UE improvement was strongly linked to network structure of the L DAN IPS, an important node in the attention pathway and one which directly connects to motor, language and visual regions. Cost, which denotes metabolic expenditure of signal routing and is a finite resource in the post-stroke brain, was lower in subjects with maximal improvement. Hence, the possibility exists that L DAN IPS organization helps to optimize energy expenditure of network transmission, given that change in L DAN IPS cost differed in each subject while change in L SMA responded consistently throughout the group. Taken together, although motor, language and visual areas appeared to be a focus of regional activation related to tDCS, motor behavior overall appeared to be most related to the connectomic arrangement of a large-scale attention network. We conclude that attention potentially represents a

◂**Figure 2.** (**a**–**d**) Averaged connectivity for 164 brain atlas regions in the stroke stim group (n = 10) are arranged in descending order. Each bar represents one region of the atlas (error bars removed for clarity). Each region is color-coded to the following functions: attention (orange), sensorimotor (green), language (magenta), visual (blue), and other (purple). These depict averaged values at the (**a**) pre-stimulation, (**b**) intra-stimulation, and (**c**) post-stimulation timepoints. (**d**) The difference in mean connectivity from pre- to post-stimulation for the stroke stim group (n = 10) is illustrated, with L SMA displaying the highest positive change in connectivity. Red boxes indicate four areas with statistically significant change with stimulation. (**e**) Subjects with a right-sided anode are represented in blue, while those with left-sided anode are shown in purple. The left column corresponds to the stroke group (N = 20) and the right column to the healthy control group (N = 20). Filled-in shapes denote subjects in the sham group. The x-axis displays the mean connectivity for the L SMA, ranging from positive to negative values. (**f**) Sagittal brain slices and connectomes illustrate L SMA connectivity changes from pre- to post-stimulation in two individual subjects. The top example represents a subject from the stroke stim group, while the bottom depicts a subject from the stroke sham group. Darker blue signifies higher connectivity, while a more translucent blue indicates lower connectivity. (**g**) The mean connectivity of the L SMA to all other 163 regions of interest were computed and compared between the pre-, intra-, and post-stimulation phases (see Supplementary Table 2 for all 4 areas with significant changes).

top-down organizing influence on stroke recovery, preserving energy metabolism while maintaining executive signal routing efficiency throughout the remaining network of lower level areas.

Key steps in the attention system were highlighted by Posner and colleagues who observed that patients with parietal lesions have difficulty disengaging and re-engaging visual cues[19]. Building on this foundation, Corbetta and Shulman argued that two segregated networks, identified as dorsal and ventral pathways, are involved in allocating attentional resources and detecting novel stimuli, respectively[20]. The parietal lobe itself is bisected by an intraparietal sulcus, which, along with the frontal eye fields, is integral to the dorsal attention network (DAN). Conversely, the inferior parietal lobule and inferior frontal gyrus play key roles in the ventral attention network (VAN). Since the early 1990s, investigators have attributed reduced motor recovery in stroke patients to deficits in attentional factors[21]. Other studies have found that attentional capabilities in stroke correlate with motor recovery, such that the ability to be attentive significantly and positively correlates with motor recovery[22]. Cheng et al. found that increased functional connectivity between the left and right DAN resulted in improved motor performance in chronic subcortical stroke patients[23]. This insight has led to the development of novel clinical approaches, such as attention process training (APT)[22], specifically designed to help stroke patients allocate attentional resources more effectively by distinguishing between valuable stimuli and distractions.

Outcomes comparable to rehabilitation have been observed among stroke patients using neuromodulation, where heightened attention levels have been linked to enhanced motor task proficiency[24]. For example, Coffman et al. recruited healthy individuals and administered an attentional task, followed by the application of tDCS and subsequent delayed attentional testing[25]. Subjects received either 0.1 or 2.0 mA for 30 min. They found a higher proficiency in the tasks correlated with increased attention. Nevertheless, Lema et al. conducted a randomized single-blinded crossover trial in healthy controls with the aim of enhancing attentional network efficiency via the use of tDCS and transcranial Random Noise Stimulation (tRNS)[26]. Stimulation was applied over the DLPFC during an attentional task. Though tRNS significantly enhanced the attention network, tDCS did not[26]. Consequently, the role of tDCS in promoting sustained attention during stroke rehabilitation remains unclear, notwithstanding results of the present study showing that DAN network architecture is linked to motor improvement. Also notable is that the Harvard–Oxford and Automated Anatomical Labeling (AAL) atlases used in the present study do not contain a specific segmentation for the VAN. We have instead considered IFG, a key VAN node, as a surrogate for this network. One interesting hypothesis is that the DAN and VAN may scale functionally according to ongoing motor and cognitive demands, given that these networks have access to and can organize large cortical and subcortical networks to recover compromised functions. While the functional lateralization of the VAN is well documented, little is known about the specific functional organization of the left DAN. Corbetta el al., reported that the VAN is primarily lateralized to the right hemisphere in healthy controls[20]. However, when examining stroke patients, they observed a shift in the lateralization within both attention networks. Left lateralization in multiple domains predominated for stroke subjects in our study regardless of stimulation status. This aspect of attention in stroke would be interesting to explore in future studies.

Tasks related to finger tapping have been repeatedly used in stroke research to quantify motor ability and as an assessment to better understand functional outcomes[27,28]. This task has been shown to increase activation in the left supplementary motor area (SMA) of stroke patients, similar to our results[29]. In our study, subjects were instructed to perform the task as fast and accurately as possible. We observed that finger sequencing movements resulted in left SMA functional connectivity increase after (but not during) tDCS activation for 10 min, suggesting a priming effect by the stimulation. Subjects receiving sham stimulation also underwent tDCS for 60 s, though L SMA activation was not seen in that group, implying stimulus duration as the primary catalyst. Nonetheless, L SMA activation did not independently correlate with FMA-UE change in either group as has been speculated in prior studies. We observed that FMA-UE change was most directly related to graph properties of large-scale attention networks, which may act to functionally integrate cognitive and motor areas during recovery. SMA is itself a motor integrative area, receiving inputs from basal ganglia, thalamus and cerebellum[24]. Engagement of these areas has been directly linked to improvements in FMA-UE[30]. We conjecture that DAN may be exerting top-down influence on a hierarchically organized network of motor and cognitive regions, the next level of which may possess some level of integrative capabilities that themselves receive multi-domain inputs from lower level areas.

Stimulation of primary motor cortex resulting from tDCS electrodes positioned over the sensorimotor area is an assumption that has rarely been challenged. In contrast, Holmes et al. utilized transcranial magnetic

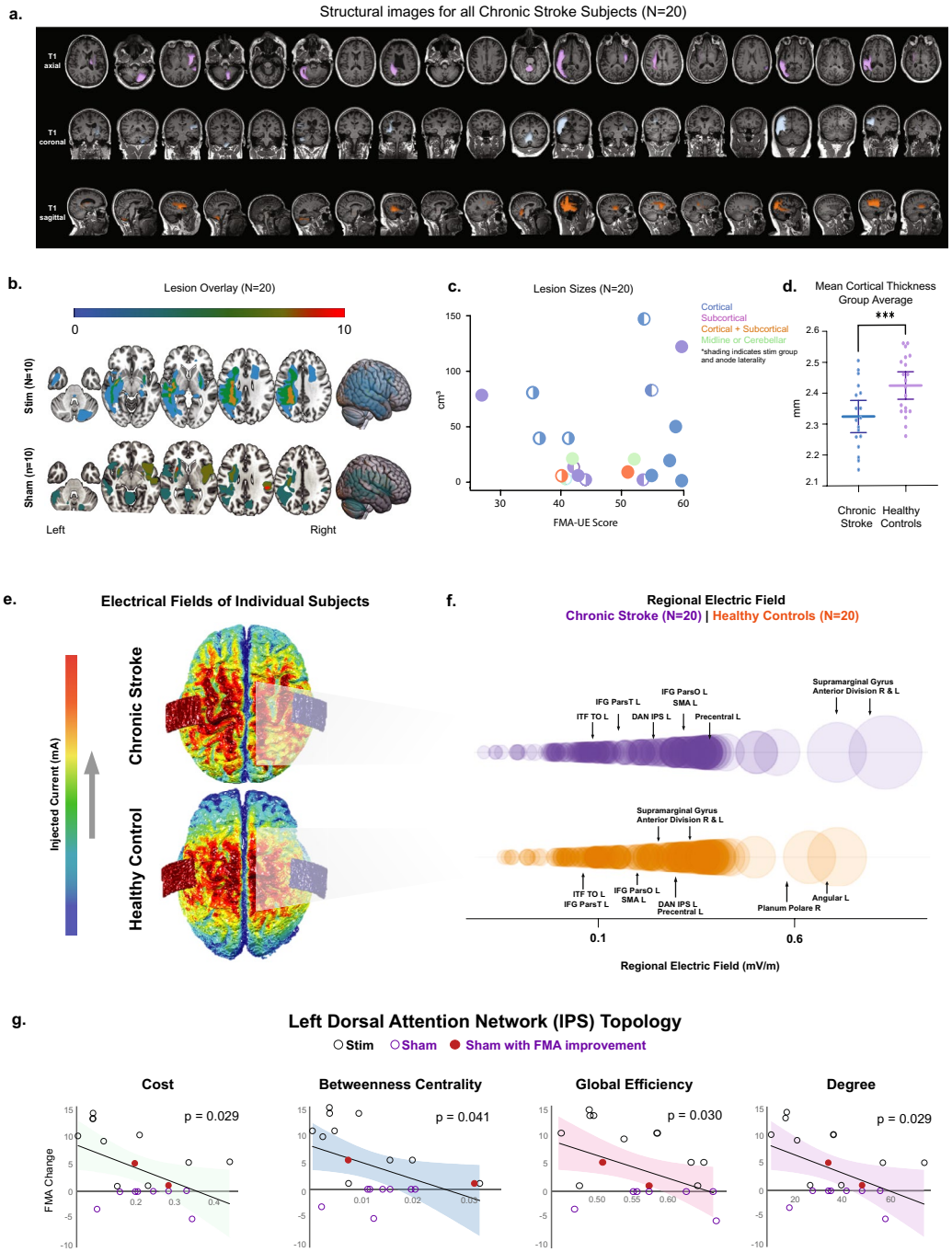

Figure 3. (**a**) Each stroke subject's T1-weighted scan is shown in axial, coronal, and sagittal orientations in order of randomization and the lesion color coded by a board-certified neuroradiologist. (**b**) Lesion overlays for the stroke stim and stroke sham groups are represented. (**c**) Lesion sizes for each individual stroke subject are shown as a function of FMA-UE score. The color of the data points corresponds to the stroke location: cortical, subcortical, cortical and subcortical, and midline or cerebellar stroke. Solid data points represent sham group subjects, while data points that are partially filled denote the stimulation group. The filled portion of these symbols reflects anode placement laterality. (**d**) A comparison of mean whole-brain cortical thickness revealed a statistically significant difference between chronic stroke subjects and healthy controls. (**e**) Models illustrating the dispersion of the electric field are shown for one stroke subject *(top)* and one healthy control *(bottom)* with roughly equal current densities. (**f**) Atlas-based electric fields (EF) were calculated for each subject. Average EF (y-axis) is shown as a function of circle diameter for chronic stroke *(purple)* and healthy control *(orange)* subjects. (**g**) Displays linear regression results correlating the pre-stimulation graph theory metrics for the left Dorsal Attention Network's (DAN) Intraparietal Sulcus (IPS) with changes in the Fugl-Meyer Assessment Upper Extremity (FMA-UE) scores for both the stroke stimulation and sham groups. Graph theory metrics examined are illustrated below the regressions, including degree, betweenness centrality, global efficiency, and cost, with lines denoting edges and spheres as nodes. P-values are fdr-corrected.

stimulation (TMS) of the supramarginal gyrus instead of motor cortex and found motor evoked potentials consistent with direct M1 stimulation[31]. This suggests that transcranially applied current may reach motor cortex via a number of routes. The supramarginal gyrus, which is located in the inferior parietal lobe (Brodmann area 40), exhibited the highest EF strength in our stroke sample (Fig. 3f). While our study did not directly test various montages, our results imply that attention networks located near this region could have been activated along with motor and pre-motor areas, including SMA.

Topological reorganization in the brain after stroke is not well understood[32]. Almeida et al. explored graph theory as a way to correlate FMA-UE improvement in a chronic stroke population[33]. In this observational study, investigators examined patients one and three months after first-ever infarct with structural imaging. They discovered that changes in betweenness centrality (BC) of the SMA and primary sensory cortex significantly correlated with change in FMA-UE. BC is a graph feature related to the fraction of short path lengths through a given node and is a surrogate for more efficient network function. In that study, as BC improved, change in FMA-UE also improved. In neurodegenerative diseases such as Alzheimer's, graph theory has been used to anticipate early clinical manifestations of the disease. In a multi-national study by Vermunt et al., a decreased number of clusters and loss of small worldness were present in patients over a decade prior to developing symptoms[34]. Small worldness is another fundamental concept in network neuroscience that denotes high clustering within interconnected modules and low average path length (i.e. short distances) between modules[35]. We argue that stroke is unique among disorders of the nervous system, since small worldness declines as symptoms in neurodegenerative disorders increase while stroke recovery can progress even in the context of relatively disorganized network configurations[34]. In our study, change in betweenness centrality was the most frequent network feature among those linked to FMA-UE change (Fig. 3g). Nevertheless, degree of FMA-UE improvement increased as pre-stimulus betweenness centrality attenuated. This argues against recovering network modularity (i.e., small worldness) as a driver of motor improvement and aligns more with the relatively disorganized connectomic topology observed in our cohort. In a recent review, Seguin et al. labels these types of networks parametric models, which use a number of less efficient rerouting strategies in order to avoid the unacceptably high costs of random signal propagation[36]. Accordingly, linear transmission, biased random walks and shortest path ensembles, the mainstays of parametric network modeling, can achieve very stable transmission rates using tradeoffs between metabolic cost, a premium in the post-infarcted brain, and targeting efficiency.

A number of study limitations provide important context to the interpretation of our findings. First, the small sample sizes of each group precluded a wider range of impairments among the stroke cohorts. For example, our sample of stroke subjects had an average baseline FMA-UE of 47, placing them in the mild to moderate impairment categories. Moreover, the stroke sham group in particular displayed milder motor impairment than the stroke stim group. For FMA-UE measurements, this introduces the possibility of a ceiling effect wherein subjects with pre-experimental mild impairment (i.e., FMA-UE near or at the highest score) have less room for improvement; for the nine-hole peg test, the opposite is true. A potential floor effect exists wherein milder subjects may not be able to reduce times any further from baseline. Future studies that include mildly affected stroke subjects (in addition to healthy subjects) may consider alternative assessment tools without such an effect. Also, prior studies have shown inconsistent results in the efficacy of tDCS to improve motor recovery in patients with severe strokes (e.g. an FMA-UE of <25) and those with extensive damage to the corticospinal tract[37–39]. Inclusion criteria for studies involving tDCS in behaving chronic stroke subjects will have to balance these factors carefully. Age is an additional variable that can affect tDCS efficacy. In a review assessing motor and cognitive influence of tDCS as a function of age, Perceval et al. reported that identical montage configurations can have opposite effects on young and old adults[40]. In addition to age, differences in stroke location have been shown to influence effect of tDCS as an independent factor. In our cohort, posterior circulation territory infarcts were more prevalent in the sham group. Interestingly, posterior, rather than anterior, infarcts were identified in a meta-analysis by Zhao et al. as more responsive to tDCS in treating dysphagia[41]. Many of the studies highlighted here did not report cognitive testing results, leaving a notable gap in our understanding. In fact, it is noteworthy that two recent interventional clinical trials for chronic stroke—VNS-REHAB and EDEN—also did not include cognitive outcomes in their reports[42,43]. Our findings may spur inclusion of such metrics in the design of future clinical studies. In addition to the testing instruments used, the study's single-blind design may be a limitation, though any placebo effect should have manifested in the healthy control group as well, which was not observed. Another fundamental challenge in studies recruiting stroke subjects is wide variability in stroke location, type, and lesion size. While lesion size did not show significant differences between the stroke stim and sham groups, the study did include subjects with different stroke types. This diversity in stroke territory underscores the complexity of drawing generalized conclusions. Finally, although the current study is underpowered relative to a randomized controlled design, our results demonstrated the intriguing possibility that functional neuroimaging could reveal topological features that relate to potential for improvement in patients with stroke.

Methods

This study was conducted at the Medical University of South Carolina (MUSC) following Institutional Review Board (pro000120319) approval. All subjects provided informed consent. The research described herein was performed in accordance with the Declaration of Helsinki as well as local guidelines and regulations.

Study design

The MUSC Registry for Stroke Recovery (RESTORE), a database of stroke survivors and healthy controls, was utilized for subject recruitment. A total of 3713 records were accessible from the database. Among the 313 individuals in the chronic stroke phase (≥ 6 months after most recent infarct), 38 were found to be ineligible due to history of seizures or other neurological conditions. A subset of 275 individuals underwent screening via phone

calls; 191 were successfully screened and deemed eligible to proceed. Twenty-two subjects were successfully scheduled for in-person study visits; two of the scheduled individuals were later deemed ineligible due to missed in-person appointment and/or MRI incompatibility. See Table 2 for screening and recruitment information for the stroke group (N = 10, active tDCS and N = 10, sham tDCS, Supplementary Fig. 2). NIH Stroke Scale (NIHSS) data were extracted from each chronic stroke subject's electronic medical record and were missing for 1 active and 4 sham subjects.

Inclusion criteria for stroke subjects consisted of the following: 18 years of age or older; hemiparesis lasting 6 months or longer prior to enrollment due to cerebral ischemic infarct or hemorrhage as documented by a board-certified neurologist; ability to open and close the hemiparetic hand. Potential subjects were excluded if they met one or more of the following criteria: having received Botulinum toxin (Botox) injections to the affected upper extremity in the past 3 months; inability to raise and outstretch either upper limb; medication use at the time of study that could interfere with tDCS, including but not limited to carbamazepine, flunarizine, sulpiride, rivastigmine, or dextromethorphan; other co-existent neuromuscular disorders (pre- or post-stroke) affecting upper extremity motor function; other neurological disorders (pre- or post-stroke) affecting subjects' ability to participate in the study; pregnancy; presence of scalp injury or disease; prior history of seizures; prior intracranial surgery; prior brain radiotherapy; prior history of intracranial tumor; intracranial infection or cerebrovascular malformation; metal in the head or neck; and any other contraindications to MRI. The criteria for selecting healthy controls included having no contraindications to MRI and being at least 18 years old. The exclusion criteria for this group were identical to those used for the chronic stroke group. Between December 2022 and July 2023, 40 subjects who satisfied all criteria were recruited. See Tables 1 and 2 for overall study sample demographics.

Randomization and blinding

Subjects in the study were assigned to either a stimulation or sham group using a pseudorandomization procedure. This involved paired matching by randomizing a subject to one group and then assigning the next consecutive subject to the opposite group. The study was single-blinded. Subjects were not informed of group assignment. The sham group underwent a placebo procedure that mimicked actual stimulation by providing sensory feedback during the initial ramp-up and final ramp-down periods.

Stimulation parameters

tDCS (Soterix Medical INC, Woodbridge, NJ) was delivered through two 5 cm × 3 cm EASY pads (Soterix Medical INC, Woodbridge, NJ) that were soaked in 0.9% NaCl and placed over the C3 and C4 regions, which approximate primary motor cortex in the 10/20 EEG International System. For stroke subjects, the anode was placed over the hemisphere contralateral to the hemiparetic side (i.e., ipsilesional or affected side). For healthy controls, the anode was randomized to the hemisphere contralateral to the hand used for the MRI task. All subjects were blinded to tDCS delivery (stimulation vs sham). Subjects were not asked about their allocation to the stimulation or the sham group. Though this questionnaire could have provided validity to the randomization paradigm, this "end-of-study guess" method has faced criticism for its lack of sensitivity as an effective measure. Additionally, concerns have been raised that subjects' judgements on tDCS blinding may be swayed by external and subconscious factors, such as memory recall or their proficiency or difficulty in performing a given task[44,45]. Montage placement was identical for all subjects. The stimulation period for the active group lasted 10 min. The device ramped to the target amplitude over a period of 30 s; an identical period was used for the ramp down. Sham subjects received 60 s of stimulation (the time it took the device to ramp to 2 mA and immediately ramp back down to 0 mA).

MRI acquisition parameters and motor testing

All subjects were imaged using a Siemens 3.0 Tesla MRI scanner with 32-channel head coil at the MUSC Center for Biomedical Imaging. MRI sequence parameters included the following: T1-weighted MPRAGE scan (192 slices per slab, 1.0 mm thick, TR = 2300 ms, TE = 2.26 ms, flip angle = 8°, voxel size 1.0 × 1.0 × 1.0 mm; FoV read = 256 mm); T2-FLAIR scan (TR = 9000 ms, TE = 91 ms, FoV read = 192 mm, flip angle = 180°, voxel size = 0.5 × 0.5 × 3.0 mm), diffusion kurtosis scan[46] (54 slices, slice thickness = 2.5 mm, TR = 3600 ms, TE = 85 ms, multi-slice mode = interleaved, FoV read = 220 mm, voxel size = 2.5 × 2.5 × 2.5 mm3, b-value 1 = 0 s/mm^2, b-value 2 = 1000 s/mm^2, b-value 3 = 2000s/mm^2, and six rs-fMRI sequences (7 min and 4 s each, slice thickness = 3.0 mm, TR = 1110 ms, TE = 30.0 ms, FoV read = 192 mm, 51 slices, flip angle = 65°, voxel size = 3.0 × 3.0 × 3.0 mm^3). Three rs-fMRI sequences and one DKI sequence were completed before and after stimulation.

Upon obtaining consent, the FMA-UE was administered to assess motor function in both the left and right limbs. Furthermore, a subset of subjects underwent the nine-hole peg test for both limbs. For this test, subjects were instructed to use one hand at a time (non-paretic hand first) to pick up the pegs one-by-one and place them in the holes. Both the FMA-UE and nine-hole peg test were administered before and after the scanning session. During the scanning session, subjects performed a finger-tapping task while inside the scanner—before, during, and after tDCS. The task consisted of 5 individual button presses in a pre-determined sequence repeated as many times as possible for 2 min. The same 5-digit sequence was used for all subjects; only correct sequences were counted.

Imaging preprocessing and functional connectivity

Raw DICOM images were converted to NIFTI format using MRIcroGL (McMausland Center for Brain Imaging, University of South Carolina, v1.2.2022). Spatial and temporal pre-processing were performed using the Functional Connectivity (CONN) Toolbox[47] (The Gabrieli Lab, McGovern Institute for Brain Research, Massachusetts

Institute of Technology, v.2017.f1) and Statistical Parametric Mapping (SPM) software (Functional Imaging Laboratory, UCL Queen Square Institute of Neurology, London, UK, v12) running in MATLAB (The Mathworks Inc, Natick, MA, USA, v2022b) as implemented by Nieto-Castanon[47]. Functional volumes underwent realignment, slice-timing correction, smoothing, segmentation, and normalization to MNI space using the normalized EPI template image in CONN and a spatial Gaussian smoothing kernel of 8 mm. A total of 164 brain regions were parcellated in an unbiased fashion using the Harvard–Oxford and Automated Anatomical Labeling (AAL) atlases. To estimate functional connectivity, seed-to-voxel analyses were completed for all subjects; seed-based connectivity (SBC) matrices were then exported to MATLAB. As defined in the CONN toolbox manual, the SBC matrix defines seeds in the brain based on the atlas labels, designates them as ROIs, extracts time-series from each region and computes a correlation analysis of the region to all other voxels in the brain. Seed-based functional connectivity was calculated using the equations below:

$$r(x) = \frac{\int S(x,t)R(t)dt}{(\int R^2(t)dt \int S^2(x,t)dt)^{1/2}}$$

$$Z(x) = \tanh^{-1}(r(x))$$

r represents the map of the Pearson correlation coefficients, while S represents the BOLD time series for each voxel. R signifies the average BOLD time series within the seed (x) that was selected over time t (https://web.conn-toolbox.org/fmri-methods/connectivity-measures/seed-based). In order to derive averages across subjects, the following equation was used to achieve Fisher transformations, converting r-values to z-scores with a normal distribution: $\tanh^{-1}(r(x))$.

FreeSurfer and lesion calculation

FreeSurfer[33] (Athinoula A. Martinos Center for Biomedical Imaging, Massachusetts General Hospital, and Harvard Medical School, version 7.1.0) was used to calculate surface-based morphometry values. Values were computed for white matter volume, cortical gray matter volume, mean cortical thickness, supratentorial volume (both with and without ventricles), and intracranial volume. Stroke lesions were hand drawn using MRIcroGL (McMausland Center for Brain Imaging, University of South Carolina, v1.2.2022). Lesion location was confirmed by a board-certified neuroradiologist (MY). Lesion size was calculated using NiiStat (McCausland Center for Brain Imaging, University of South Carolina, SC; https://github.com/neurolabusc/NiiStat) and SPM12 (version 7487) (Functional Imaging Laboratory, Wellcome Trust Centre for Neuroimaging Institute of Neurology, University College London; http://www.fil.ion.ucl.ac.uk/spm/software/spm12/).

ROAST

ROAST, a MATLAB toolbox, was employed to compute the voltage and electric field values for the chronic stroke stim and sham subjects. Input parameters included T1-weighted scans for each subject and electrode details such as size, location, and stimulation strength. Structural scans underwent segmentation into tissue types (e.g., bone, CSF, gray matter, white matter), and simulated electrodes were positioned according to the predefined parameters. Finite element mesh models were generated for each stroke subject. The maximum electric field strength for each brain region was determined using MNI coordinates. Additionally, skull and scalp thicknesses at the C3 and C4 locations were computed in subject-space. T1 scans were not available for healthy subjects.

Graph theory calculations

The graph theory analyses conducted within the CONN Toolbox encompassed the following metrics: degree, cost, average path length, clustering coefficient, global efficiency, local efficiency, and betweenness centrality. In the graph theory equations below, notations followed by an 'i' indicate a specific node. As defined in the CONN toolbox manual, degree and cost were calculated using the following[48,49]:

$$d_i = \sum_j A_{i,j}$$

$$d = \frac{\Sigma_i d_i}{N}$$

$$c_i = \frac{\Sigma_j A_{i,j}}{N-1}$$

$$c = \frac{\Sigma_i c_i}{N}$$

The total number of nodes are denoted by N in the current and all following equations. A corresponds to the adjacency matrix that is calculated by thresholding the ROI-to-ROI matrix, whereas c is the cost and d is the degree of each node.

Average path length was calculated using the equation below:

$$L_i = \frac{\Sigma_{j\epsilon\Omega i} D_{i,j}}{N_i - 1}$$

$$L = \frac{\Sigma_i L_i}{N}$$

L is the average of the path distance, and D is the shortest path distance.
Clustering coefficient was calculated using the equation below:

$$CC_i = \frac{\Sigma_{j,k\in\Gamma i} A^{(i)}_{j,k}}{N}$$

$$CC = \frac{\Sigma_i CC_i}{N}$$

CC corresponds to the clustering coefficient of a graph and individual nodes, representing local integration.
Global efficiency was calculated using the equation below:

$$GE_i = \frac{\Sigma_{j\neq i} 1/D_{i,j}}{N - 1}$$

$$GE = \frac{\Sigma_i GE_i}{N}$$

GE corresponds to the global efficiency of each graph and individual nodes, representing global connectedness.
Local efficiency was calculated using the equation below:

$$LE_i = \frac{\Sigma_{j\neq k\epsilon\Gamma i} 1/D^{(i)}_{j,k}}{d_i(d_i - 1)}$$

$$LE_i = \frac{\Sigma_i LE_i}{N}$$

LE corresponds to the local efficiency of each graph and individual nodes, representing the local coherence among nodes with their neighboring nodes.

Betweenness centrality was calculated using the equation below:

$$BC = \frac{\Sigma_i BC_i}{N}$$

BC corresponds to betweenness centrality between a graph and individual nodes, representing the proportion of the shortest path of a node between two other nodes. P corresponds to the shortest path between nodes (https://web.conn-toolbox.org/fmri-methods/connectivity-measures/seed-based).

Statistical analysis

Power analysis demonstrated a Cohen's d-test of 0.8 (regression, $1-\beta = 0.80$, $\alpha = 0.05$) using a sample size of 80 chronic stroke subjects (G*Power version 3.1.9.7, Department of Experimental Psychology, University of Düsseldorf, Germany). For this study, we enrolled 40 subjects to demonstrate feasibility of the combined tDCS-fMRI methodology.

All data were analyzed in MATLAB (MathWorks, Natick, MA, USA, v2022b). Group mean errors were reported as standard deviation. Pearson's Chi-square test, denoted by χ^2, was used to compare categorical variables between groups. A paired or unpaired two-tailed t-test, denoted by the test (t) statistic, was used to compare group means among repeated or independent samples, respectively. To survey all 164 ROIs, repeated-measures ANOVA, denoted by F, was used to determine differences between connectivity timepoints (pre-, intra-, and post). Significance was set at $p < 0.05$ for all categorical and means comparison testing. Tukey's test was used for post-hoc comparisons. To provide a more focused analysis, we examined p-values from left-sided ROIs involved in motor, language and visual areas only given that we observed a left-lateralized predominance in our connectivity data. In this sub-analysis, all right-sided and non-lateralized ROIs (e.g., cerebellar vermis I–X) were excluded (total left-sided ROIs were 55 out of 164 ROIs and included the left dorsal attention network IPS and FEF). To control for Type I errors in this group, false discovery rate (fdr) testing was employed ('mafdr' function in MATLAB, threshold of < 0.05). FDR-corrected values are listed in Supplementary Table 2. FDR-corrected values for cortical thickness (average of 30 ROIs) were based on t-test results comparing stim vs sham stroke subjects.

It is well known that graph theory metrics suffer from test–retest reliability, and standard multiple comparison approaches used to threshold significant effects are highly unpredictable, including fdr. Thus, we used a modified multi-threshold permutation correction method to optimize sensitivity to the small group effects observed in our data[50]. Using the implementation by Drakesmith et al., we calculated a random distribution of p-values using the experimental p-value ranges for each metric. We then filtered the distribution to those p-values falling below the 99th% confidence interval based on the mean of the random data set; this confidence interval was

considered the new significance threshold. The new distribution was compared to those from a 1000 randomly generated p-value distributions with accompanying 99th% confidence intervals. The filtered distribution from the more conservative threshold was then corrected using fdr. Figures were generated in GraphPad Prism (GraphPad Software Inc., La Jolla, CA, USA, v8.0.2).

Data availability

The datasets generated and/or analysed during the current study are available from the corresponding author on reasonable request.

Received: 13 February 2024; Accepted: 12 August 2024
Published online: 20 August 2024

References

1. McDonald, M. W. *et al.* Cognition in stroke rehabilitation and recovery research: Consensus-based core recommendations from the second Stroke Recovery and Rehabilitation Roundtable. *Int. J. Stroke* **14**, 774–782 (2019).
2. Barrett, A. M. & Muzaffar, T. Spatial cognitive rehabilitation and motor recovery after stroke. *Curr. Opin. Neurol.* **27**, 653–658 (2014).
3. VanGilder, J. L., Hooyman, A., Peterson, D. S. & Schaefer, S. Y. Post-stroke cognitive impairments and responsiveness to motor rehabilitation: A review. *Curr. Phys. Med. Rehabil. Rep.* **8**, 461–468 (2020).
4. Anderlini, D., Wallis, G. & Marinovic, W. Language as a predictor of motor recovery: The case for a more global approach to stroke rehabilitation. *Neurorehabil. Neural Repair* **33**, 167–178 (2019).
5. Joy, M. T. & Carmichael, S. T. Encouraging an excitable brain state: Mechanisms of brain repair in stroke. *Nat. Rev. Neurosci.* **22**, 38–53 (2021).
6. Hertrich, I., Dietrich, S., Blum, C. & Ackermann, H. The role of the dorsolateral prefrontal cortex for speech and language processing. *Front. Hum. Neurosci.* **15**, 645209 (2021).
7. La Corte, E. *et al.* The Frontal Aslant Tract: A systematic review for neurosurgical applications. *Front. Neurol.* **12**, 641586 (2021).
8. Hu, J. *et al.* Abnormal brain functional and structural connectivity between the left supplementary motor area and inferior frontal gyrus in moyamoya disease. *BMC Neurol.* **22**(1), 179 (2022).
9. Brown, C. E., Aminoltejari, K., Erb, H., Winship, I. R. & Murphy, T. H. In vivo voltage-sensitive dye imaging in adult mice reveals that somatosensory maps lost to stroke are replaced over weeks by new structural and functional circuits with prolonged modes of activation within both the peri-infarct zone and distant sites. *J. Neurosci.* **29**, 1719–1734 (2009).
10. Kwakkel, G. Understanding dynamics of motor recovery after stroke. *Ann. Phys. Rehabil. Med.* **56**, e177 (2013).
11. Riley, E. A., Verblaauw, M., Masoud, H. & Bonilha, L. Pre-frontal tDCS improves sustained attention and promotes artificial grammar learning in aphasia: An open-label study. *Brain Stimul.* **15**, 1026–1028 (2022).
12. Kwon, Y. H. *et al.* Primary motor cortex activation by transcranial direct current stimulation in the human brain. *Neurosci. Lett.* **435**, 56–59 (2008).
13. Antal, A., Polania, R., Schmidt-Samoa, C., Dechent, P. & Paulus, W. Transcranial direct current stimulation over the primary motor cortex during fMRI. *Neuroimage* **55**, 590–596 (2011).
14. Kwon, Y. H. & Jang, S. H. The enhanced cortical activation induced by transcranial direct current stimulation during hand movements. *Neurosci. Lett.* **492**, 105–108 (2011).
15. Hummel, F. & Cohen, L. G. Improvement of motor function with noninvasive cortical stimulation in a patient with chronic stroke. *Neurorehabil. Neural Repair* **19**, 14–19 (2005).
16. Langhorne, P., Coupar, F. & Pollock, A. Motor recovery after stroke: A systematic review. *Lancet Neurol.* **8**, 741–754 (2009).
17. Hunold, A., Haueisen, J., Freitag, C. M., Siniatchkin, M. & Moliadze, V. Cortical current density magnitudes during transcranial direct current stimulation correlate with skull thickness in children, adolescent and young adults. *Prog. Brain Res.* **264**, 41–56 (2021).
18. Nissim, N. R. *et al.* Through thick and thin: baseline cortical volume and thickness predict performance and response to transcranial direct current stimulation in primary progressive aphasia. *Front. Hum. Neurosci.* **16**, 907425 (2022).
19. Posner, M. I., Walker, J. A., Friedrich, F. J. & Rafal, R. D. Effects of parietal injury on covert orienting of attention. *J. Neurosci.* **4**, 1863–1874 (1984).
20. Corbetta, M. & Shulman, G. L. Control of goal-directed and stimulus-driven attention in the brain. *Nat. Rev. Neurosci.* **3**, 201–215 (2002).
21. Robertson, I. H., Ridgeway, V., Greenfield, E. & Parr, A. Motor recovery after stroke depends on intact sustained attention: A 2-year follow-up study. *Neuropsychology* **11**, 290–295 (1997).
22. Barker-Collo, S. L. *et al.* Reducing attention deficits after stroke using attention process training: A randomized controlled trial. *Stroke* **40**, 3293–3298 (2009).
23. Cheng, H. J. *et al.* Task-related brain functional network reconfigurations relate to motor recovery in chronic subcortical stroke. *Sci. Rep.* **11**(1), 8442 (2021).
24. Akkal, D., Dum, R. P. & Strick, P. L. Supplementary motor area and presupplementary motor area: Targets of basal ganglia and cerebellar output. *J. Neurosci.* **27**, 10659–10673 (2007).
25. Coffman, B. A., Trumbo, M. C. & Clark, V. P. Enhancement of object detection with transcranial direct current stimulation is associated with increased attention. *BMC Neurosci.* **13**, 108 (2012).
26. Lema, A., Carvalho, S., Fregni, F., Gonçalves, Ó. F. & Leite, J. The effects of direct current stimulation and random noise stimulation on attention networks. *Sci. Rep.* **11**, 6201 (2021).
27. Cramer, S. C. *et al.* A Functional MRI Study of Three Motor Tasks in the Evaluation of Stroke Recovery.
28. Verstynen, T., Diedrichsen, J., Albert, N., Aparicio, P. & Ivry, R. B. Ipsilateral motor cortex activity during unimanual hand movements relates to task complexity. *J. Neurophysiol.* **93**, 1209–1222 (2005).
29. Platz, T. *et al.* Impairment-oriented training and adaptive motor cortex reorganisation after stroke: A fTMS study. *J. Neurol.* **252**, 1363–1371 (2005).
30. Fries, W., Danek, A., Scheidtmann, K. & Hamburger, C. Motor recovery following capsular stroke. Role of descending pathways from multiple motor areas. *Brain* **116**(Pt 2), 369–382 (1993).
31. Holmes, N. P. *et al.* Transcranial magnetic stimulation over supramarginal gyrus stimulates primary motor cortex directly and impairs manual dexterity: Implications for TMS focality. *J. Neurophysiol.* **131**, 360–378 (2024).
32. Schlemm, E. *et al.* Structural brain networks and functional motor outcome after stroke—A prospective cohort study. *Brain Commun.* **2**, fcaa001 (2020).
33. Almeida, S. R. M. *et al.* Modeling functional network topology following stroke through graph theory: Functional reorganization and motor recovery prediction. *Braz. J. Med. Biol. Res. Rev. Bras. Pesqui. Medicas e Biol.* **55**, e12036 (2022).

34. Aerts, H., Fias, W., Caeyenberghs, K. & Marinazzo, D. Brain networks under attack: Robustness properties and the impact of lesions. *Brain* **139**, 3063–3083 (2016).
35. Hsieh, Y.-W. *et al.* Responsiveness and validity of three outcome measures of motor function after stroke rehabilitation. (2009). https://doi.org/10.1161/STROKEAHA.108.530584
36. Seguin, C., Sporns, O. & Zalesky, A. Brain network communication: Concepts, models and applications. *Nat. Rev. Neurosci.* **24**, 557–574 (2023).
37. Feng, W. *et al.* Transcranial direct current stimulation for poststroke motor recovery: challenges and opportunities. *PM R* **10**, S157–S164 (2018).
38. Chhatbar, P. Y. *et al.* Transcranial direct current stimulation post-stroke upper extremity motor recovery studies exhibit a dose-response relationship. *Brain Stimul.* **9**, 16–26 (2016).
39. Feng, W. *et al.* Corticospinal tract lesion load: An imaging biomarker for stroke motor outcomes. *Ann. Neurol.* **78**, 860–870 (2015).
40. Perceval, G., Flöel, A. & Meinzer, M. Can transcranial direct current stimulation counteract age-associated functional impairment?. *Neurosci. Biobehav. Rev.* **65**, 157–172 (2016).
41. Zhao, N. *et al.* Effects of transcranial direct current stimulation on poststroke dysphagia: A systematic review and meta-analysis of randomized controlled trials. *Arch. Phys. Med. Rehabil.* **103**, 1436–1447 (2022).
42. Baker, K. B. *et al.* Cerebellar deep brain stimulation for chronic post-stroke motor rehabilitation: A phase I trial. *Nat. Med.* **29**, 2366–2374 (2023).
43. Dawson, J. *et al.* Vagus nerve stimulation paired with rehabilitation for upper limb motor function after ischaemic stroke (VNS-REHAB): A randomised, blinded, pivotal, device trial. *Lancet (London, England)* **397**, 1545–1553 (2021).
44. Turner, C., Jackson, C. & Learmonth, G. Is the 'end-of-study guess' a valid measure of sham blinding during transcranial direct current stimulation?. *Eur. J. Neurosci.* **53**, 1592–1604 (2021).
45. Stanković, M., Živanović, M., Bjekić, J. & Filipović, S. R. Blinding in tDCS studies: Correct end-of-study guess does not moderate the effects on associative and working memory. *Brain Sci.* **12**(1), 58 (2021).
46. Jensen, J. H. & Helpern, J. A. MRI quantification of non-Gaussian water diffusion by kurtosis analysis. *NMR Biomed.* **23**, 698–710 (2010).
47. Nieto-Castanon, A. *Handbook of Functional Connectivity Magnetic Resonance Imaging Methods in CONN* (Hilbert Press, 2020). https://doi.org/10.56441/hilbertpress.2207.6598
48. Wallis, W. D. Graph theory with applications (J. A. Bondy and U. S. R. Murty). in *SIAM Rev.* **21**, 429–429 (1979).
49. van Wijk, B. C. M., Stam, C. J. & Daffertshofer, A. Comparing brain networks of different size and connectivity density using graph theory. *PLoS One* **5**, e13701 (2010).
50. Drakesmith, M. *et al.* Overcoming the effects of false positives and threshold bias in graph theoretical analyses of neuroimaging data. *Neuroimage* **118**, 313–333 (2015).

Author contributions

Study Design: C.A.S., N.C.R. Writing and figure preparation: C.A.S., N.C.R. prepared the initial draft of the manuscript and figures. Experiments: C.A.S., N.C.R. recruited and administered the study protocol. Analysis: C.A.S., N.C.R., I.H., J.M.W. performed analyses of the data. Study supervision: N.C.R., L.B., M.S.G., S.K., M.Y. Provided edits to the manuscript: D.L., I.E.H., J.J., L.B., P.G., M.Y., S.A.K., C.H., M.S.G., S.A.K, N.C.R. All authors reviewed and approved the submitted version.

Funding

Center of Biomedical Research Excellence (COBRE) in Stroke Recovery—Junior Investigator Research Project. Source: National Institutes of Health (5 P20 GM109040).

Competing interests

The authors declare no competing interests.

Additional information

Supplementary Information The online version contains supplementary material available at https://doi.org/10.1038/s41598-024-70083-5.

Correspondence and requests for materials should be addressed to N.C.R.